

Soil property and class maps of the conterminous US at 100 meter spatial resolution based on a compilation of soil point observations and machine learning

Amanda Ramcharan¹, Tomislav Hengl², Travis Nauman³, Colby Brungard⁴, Sharon Waltman⁵, Skye Wills⁶, James Thompson⁷

| | |
|---|--|
| 1 | Penn State University, University Park, PA |
| 2 | ISRIC — World Soil Information, Wageningen, Netherlands |
| 3 | US Geological Survey, Southwest Biological Science Center, Moab, Utah |
| 4 | New Mexico State University, Las Cruces, New Mexico |
| 5 | West Virginia University — GRU, Morgantown, West Virginia |
| 6 | NRCS, Lincoln Nebraska |
| 7 | West Virginia University, Morgantown, West Virginia |

Corresponding author: Amanda Ramcharan

Abstract

With growing concern for the depletion of soil resources, conventional soil data must be updated to support spatially explicit human-landscape models. Three US soil point datasets — the National Cooperative Soil Survey (NCSS) Characterization Database, National Soil Information System (NASIS), and the Rapid Carbon Assessment (RaCA) dataset — were combined with a stack of over 200 environmental datasets to generate complete coverage gridded predictions at 100 m spatial resolution of soil properties (percent organic C, total N, bulk density, pH, and percent sand and clay) and US soil taxonomic classes (291 great groups and 78 modified particle size classes) for the conterminous US. Models were built using parallelized random forest and gradient boosting algorithms. Soil property predictions were generated at seven standard soil depths (0, 5, 15, 30, 60, 100 and 200 cm). Prediction probability maps for US soil taxonomic classifications were also generated. Model validation results indicate an out-of-bag classification accuracy of 60% for great groups, and 66% for modified particle size classes; for soil properties cross-validated R-square ranged from 62% for total N to 87% for pH. Nine independent validation datasets were used to assess prediction accuracies for soil class models and results ranged between 24-58% and 24-93% for great group and modified particle size class prediction accuracies, respectively. The hybrid "SoilGrids+" modeling system that incorporates remote sensing data, local predictions of soil properties, conventional soil polygon maps, and machine learning opens the possibility for updating conventional soil survey data with machine learning technology to make soil information easier to integrate with spatially explicit models, compared to multi-component map units.

Introduction

The National Academy of Sciences has reported changes in the quality of soil and water resources have accelerated during the past decades at a rate proportional to human-induced activities and population growth (2001). With the growing concern about finite soil resources, soil scientists are now tasked with providing information that can support spatially explicit human-landscape models that can aid in preserving soil resources. This information needs to meet current requirements to estimate and manage stores and fluxes of water, carbon, nutrients, and solutes in soil. Conventional systems for mapping and

classifying soils were not designed for this purpose (Arrouays et al., 2014). Instead, a gridded product with three-dimensional estimates of soil properties is required.

The highest resolution three-dimensional soil database with conterminous coverage of the US is the vector Soil Survey Geographic database (SSURGO) and its 10 m resolution gridded equivalent: gSSURGO (Soil Survey Staff, 2016). Given this database compiles approximately 3,000 independent soil surveys varying in scale from 1:12,000 to 1:125,000 (Thompson et al., 2012), associated tabular attributes of different scales and map units comprising different numbers of soil components require spatial disaggregation, which is often not trivial at regional or national scale. Odgers et al. (2012) have produced 100 m resolution soil property maps from the US General Soil Map (STATSGO2) by combining spline fitting and weighted averaging per mapping unit. Although nominally at high spatial resolution, maps produced by Odgers et al. (2012) still reveal a relatively coarse scale of the STATSGO2 (1:250,000). Chaney et al. (2016) recently disaggregated and harmonized SSURGO components within the SSURGO database to create POLARIS — a 30 m spatial resolution map of the 50 most probable SSURGO components. Linking soil properties to POLARIS has shown to be complex due to low accuracies, hence it remains to be determined whether creating soil property maps from SSURGO component predictions is the optimal path to follow.

Acknowledging the complexities of creating gridded soil property maps from conventional soil maps, such as artificial boundaries in the data associated with geopolitical boundaries, unnamed soil components, and variation in soil properties in soil components without location of these components within the larger map unit delineation (Thompson et al., 2010; Odgers et al., 2012; Arrouays et al., 2014; Batjes 2016), we have opted here for a point data / machine learning-driven three-dimensional approach to predictive soil mapping. Machine learning algorithms such as regression trees, Cubist, and random forests have been proven useful for predictive soil mapping by Henderson et al., (2005) and Kheir et al., (2010), and then later on by Hengl et al. (2014; 2017), who have developed a fully automated framework for global soil property and class mapping called "SoilGrids". One limitation of the (global) SoilGrids system, however, is the inability to integrate detailed national data from conventional soil maps into the modeling system. Integrating national soil and environmental datasets may result in predictions with a higher accuracy than

previous SoilGrids results; which were mostly driven by remote sensing covariates. We propose a hybrid machine learning-based framework that builds three-dimensional spatial predictions from a comprehensive stack of environmental datasets available in the US, including conventional soil maps, climatic and topographic covariates, and point data. We use this framework to provide full coverage gridded information for the conterminous US which can be rapidly updated as revised observations of soil properties and classes become available. The soil property maps we produced include: bulk density, pH, percent sand, clay, percent organic C and total N at seven standard soil depths (0, 5, 15, 30, 60, 100, and 200 cm). Soil class maps include US Soil Taxonomy great group (GG) and modified Particle Size Classes (mPSC). Modified particle size classes are a functional descriptor in US Soil Taxonomy designed to combine agricultural and engineering soil particle size classification systems (Soil Survey Staff, 2010) and has been used to identify areas of similar ecological potential to aid in land management (Nauman and Duniway, 2016). In the following sections we provide model fitting, accuracy assessment results, and discuss advantages and disadvantages of our approach. All soil maps described in this paper are available under the Open Database License (ODbL) v1.0 and can be obtained from the Penn State University repository at <https://scholarsphere.psu.edu> (DOI: <https://doi.org/10.18113/S1KW2H>).

Methods and Materials

Spatial Prediction with Machine Learning

For this study, we used two types of models for generating predictions:

1. For soil class-type variables (GG and mPSC): we used the random forest method (Breiman, 2001), as implemented in the ranger package (Wright, 2016) for R (R Core team, 2016).
2. For soil property numeric-type variables: we used an ensemble of two tree-based machine learning methods: random forest (Breiman, 2001) and gradient boosting (Friedman, 2002), as implemented via the ranger package (Wright, 2016) and xgboost package (Chen and Guestrin, 2016), both available as R contributed packages (R Core Team, 2016).

variables is better one realization alone. Mulder et al. (2016) correctly recognized that, in many areas in the world, locally produced predictions of soil properties would likely be significantly more accurate than SoilGrids. Acknowledging each contributor model will have its own strength and weaknesses, we decided to combine global and local predictions rather than selecting the single best-performing model for a given situation or scenario (the traditional pursuit). No model variograms for residuals nor kriging of predictions with residuals were done as some research has shown this to be unnecessary for variables where covariates explain >60% of spatial variation (Lacoste et al., 2016, Vaysse et al., 2015, Hengl et al., 2015).

The ranger and xgboost packages were specifically selected for predictive modeling because:

- they have high prediction accuracies when modeling complex interactions among predictor variables (Cutler et al., 2007, Rodriguez-Galiano et al., 2012, Hengl et al. 2017), and
- they can be implemented in parallel, so that predictions can be generated for large volumes of pixels.

The number of trees grown in the random forest model was reduced from the default setting of 500 to minimize the risk of model overfitting. This was also done as previous research showed no significant effect on model accuracy from reducing the number of trees in the model (Latinne et al., 2001, Oshiro et al., 2012). After initial testing the number of trees grown for all models was set to 85. The train function of the *caret* package (Kuhn, 2008) was used to tune model parameters and final parameter selection was based on reducing the RMSE over 100 iterations. The parameters tuned included *eta* and *max_depth* and final values were 0.4 and 3 for soil property models. *Eta* controls the learning rate of the forest by scaling the contribution of each tree between 0 and 1, while *Max_depth* is the maximum depth of a tree. For soil property models the xgboost tuning parameters *gamma*, *colsample_bytree*, and *min_child_weight* were held constant at 0, 0.8, and 1 respectively. *Gamma* is the minimum loss reduction required to make a partition on a leaf node of a tree, *Colsample_bytree* is the fraction of columns to sample from when constructing a tree, and *min_child_weight* is the minimum number of instances set in a terminal node (Chen and Guestrin, 2016). Tuning results of *mtry*- the number of variables randomly sampled at each split in the random forest model- is reported in Supplementary Table S1.

The general spatial prediction framework is described in detail in Figure 1 and includes a number of GIS operations such as downscaling, aggregation of rasters, spatial overlay, fitting of machine learning models, generation of predictions, and data export. All processing was implemented on a 508 GB RAM high-performance server with 48 cores and 4 TB of disk space. For soil properties, model fitting and spatial prediction (values at seven standards depths) took ~12 hours per property to build models and predict; soil classes took ~14 hours to build models and generate spatial predictions.

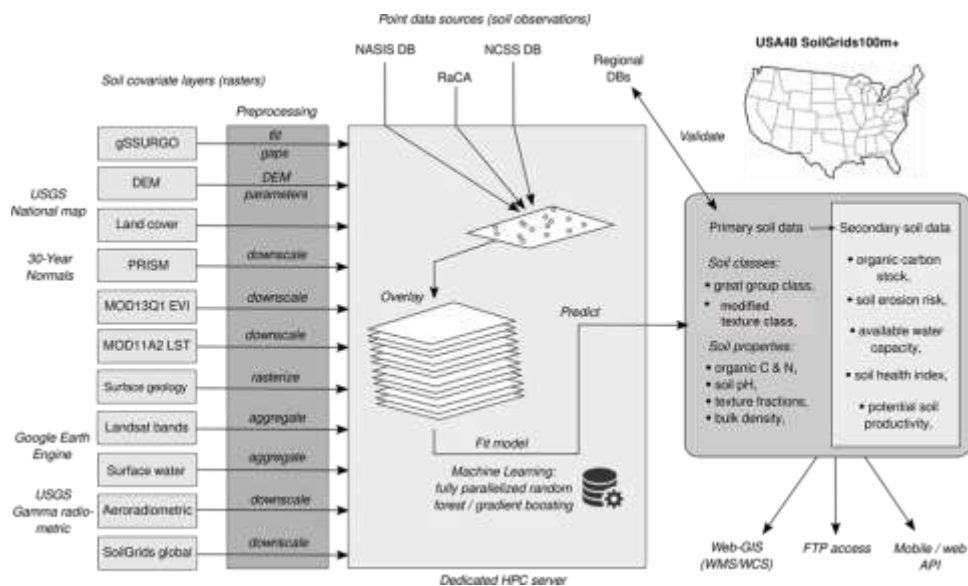


Figure 1. General data processing workflow used to generate spatial predictions at 100 m resolution (USA48 SoilGrids100m+).

Final soil properties modeled and mapped included:

- Soil organic C in % weight (% wt),
- Sand and clay in % weight (% wt),
- Bulk density of the fine earth fraction (< 2 mm) in g cm^{-3} ,
- Total N in % weight (% wt),
- Soil pH in 1:1 soil- H_2O solution,

USDA taxonomic soil classes modeled and mapped included:

- Modified particle size classes (mPSC — 78 classes),
- Soil great group (GG — 291 classes),

Input Data

For model training we used point data from three data sources:

1. National Cooperative Soil Survey (NCSS) Characterization Database,
2. National Soil Information System (NASIS), and
3. Rapid Carbon Assessment (RaCA) project.

The National Cooperative Soil Survey (NCSS) Characterization Database

The NCSS characterization database provides soil characterization data from projects performed by the Kellogg Soil Survey Laboratory and cooperating laboratories (NCSS, 2015). Beginning with the 2015 NCSS database, 34,183 pedons (213,499 horizons) were available for spatial modeling. This database was filtered to retain only soil samples that had a minimum of a site location (WGS84 coordinates) and at least one soil property observation.

The degree of completeness for each soil pedon and the available property and attribute data for each individual sample varied across the database. Most data had soil organic C, soil texture (sand, silt, clay content), and pH. For the organic C data, a linear regression based on Wills et al. (2013) was applied to Walkley-Black organic C measurements to align with total combustion carbon measurements. Data preprocessing was done to remove negative values for soil properties. Compiled soil sample data contain variation that can come from several potential error types in addition to the actual property variation. These include the level of accuracy recorded, measurement error, the date at which the sample was taken, and imprecise methods of locating sampling locations. These factors can introduce biases into the models as these differences may be confounded with changes in property or class values. Corrections can be made for some factors to reduce this possibility, as was done for organic C, but overall there is limited ability to isolate or negate the effects of these factors on derived models.

National Soil Information System (NASIS) Data

The US Department of Agriculture — Natural Resources Conservation Service (NRCS), maintains a large database of soil maps and observations called the National Soil Information System (NASIS). We utilized NASIS records made primarily during soil survey activities (separate from NCSS characterization data). These observations are mostly field observations made by scientists using transects to determine SSURGO components and build map units. Most have not been tested in a laboratory, but were described and classified to SSURGO components and US Soil Taxonomy classes (Soil Survey Staff, 1999, 2014) by experienced local soil scientists.

The most recent taxonomic classification for each observation was queried from NASIS using R (R Core Team, 2016). Soil great group (GG, e.g. "Calciargids") and particle size classes (PSC, e.g. "Loamy" or "Coarse-loamy") were then extracted from taxonomic class names. Particle size classes are one of the most consistently defined taxonomic descriptors in US *Soil Taxonomy* (Caudle et al., 2013, Duniway et al., 2010). These classes generalize the texture of a soil profile based on a representative set of depths called the control section, which is specific to different groups of soils (Soil Survey Staff, 2014). Extracted PSC were then modified (mPSC) as follows to ensure that classes more fully covered the spectrum of possible soils across the conterminous US (Nauman and Duniway, 2016). Observations of rock outcrops, which traditionally have no PSC, were labeled as such. To avoid redundancy in the taxonomic classification, Psamments (sandy soils) were assigned to a sandy class as these soils have no particle size class designation. Soils with a Lithic (i.e., shallow bedrock contact) taxonomic classification were labeled with a "Lithic" modified particle size class. Histosols (organic soils), which traditionally have no PSC, were assigned to an "Organic" modified particle size class. These processing steps resulted in 328,380 GG observations and 308,291 mPSC observations that were used as training data for building soil class models (see Figure 2).

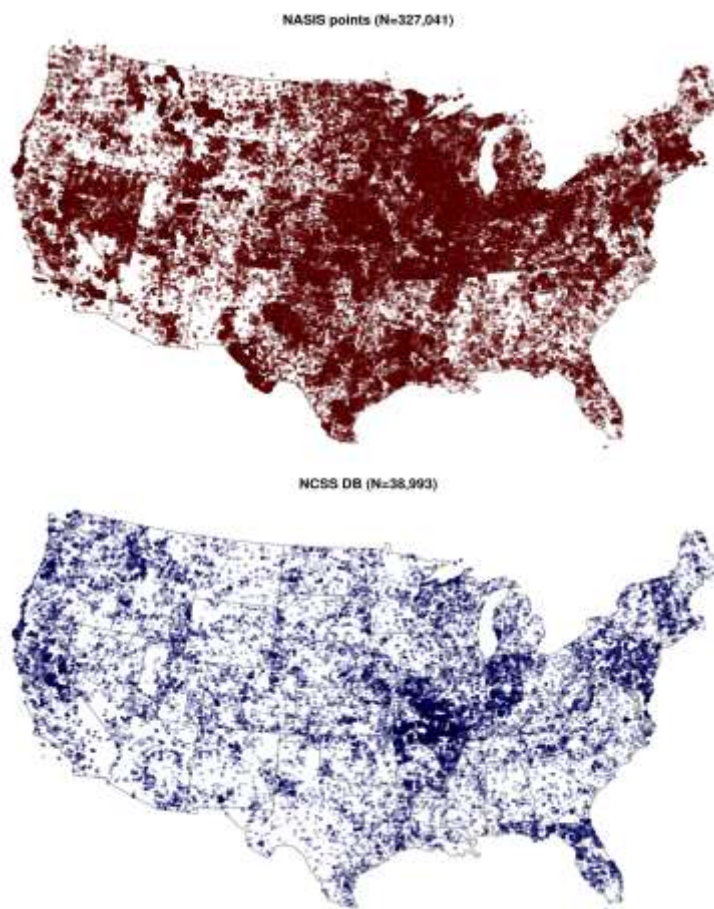


Figure 2. Maps of points used to train models red — NASIS soil class points, blue — NCSS database and RaCA points (combined).

The Rapid Carbon Assessment (RaCA) dataset

The NRCS Rapid Carbon Assessment (RaCA) project was conducted to capture information on the carbon content of soils across the conterminous US (Soil Survey Staff and Loecke, 2016). A multi-level stratified random sampling scheme was created to maximize spatial sample coverage. RaCA consisted of 31,215 pedon observations with organic C, total N, and bulk density measurements (when possible) in the 0–50 cm profile range. Soil organic C and total N measurements were performed according to standard Kellogg Soil Survey Laboratory methods (Soil Survey Staff, 2014). The RaCA dataset was combined with the NCSS database for predicting soil properties.

Soil Covariates

We used a range of geospatial datasets relevant to soil formation to build a stack of environmental covariates for predictive soil modeling. Each environmental covariate was either sourced at 100 m resolution or a resampling method was applied to convert data to 100 m resolution (e.g. cubicspline was applied to PRISM datasets to convert from 800 m to 100 m). Examples of the environmental covariates are shown in Figure 3 and a detailed summary of the datasets, sources, and resampling methods are made available on Github (https://github.com/aramcharan/US_SoilGrids100m).

The environmental covariates included:

- *DEM-derived covariates*: Ten terrain attributes were derived from a conterminous 100 m digital elevation model (DEM) for the US (The National Map, 2013) using SAGA GIS software (Conrad et al. 2015). These included: elevation, slope gradient, profile curvature, multiresolution index of valley bottom flatness (MRVBF), surface roughness, valley depth, negative topographic openness, positive topographic openness, Melton ruggedness number, SAGA wetness index, and topographic position index.
- *PRISM climate covariates*: PRISM 30-year normal climate surfaces covering the period 1971-2010 included precipitation, mean temperature, minimum temperature, maximum temperature, mean dew point temperature, minimum vapor pressure deficit, and maximum vapor pressure deficit (Daly et al., 2008). Nineteen bioclimatic indices (e.g. annual diurnal range, total precipitation in the driest quarter, average temperature in the driest quarter) derived from PRISM normal datasets by O'Donnell and Ignazio (2012) were also included.
- *MODIS land products*: Satellite imagery datasets derived from 35 years of MODIS data included six long-term averaged bi-monthly mean and standard deviation Enhanced Vegetation Index (EVI); six long-term averaged bi-monthly mean surface reflectances for MODIS bands four (NIR) and seven (MIR); 24 long-term averaged monthly mean daytime and nighttime surface temperature; 12 long-term averaged monthly cloud cover datasets of twice-daily remote sensing-derived cloud observations (LP DAAC, 2014).

- *Landsat 30 m resolution products*: Landsat (cloud-free) NIR, SWIR bands, gamma radiometric images (Hansen et al., 2013), long-term surface water occurrence (Pekel et al., 2016) and bare ground images were aggregated from 30 m to 100 m using the averaging algorithm in GDAL (Warmerdam, 2008).
- *SoilGrids250m*: SoilGrids250m (Hengl et al., 2017) soil property maps were included in the covariate stack. The original maps were downsampled to 100 m resolution using bicubic resampling in GDAL (Warmerdam, 2008).
- *Additional environmental covariates*: These included: land cover classes for the year 2011 (USGS, 2011), US potential natural vegetation (Kuchler, 1964), historical natural fire regime classes (Fire Sciences Laboratory, Rocky Mountain Research, 2001), and aeroradiometric grids (Duval et al., 2005).

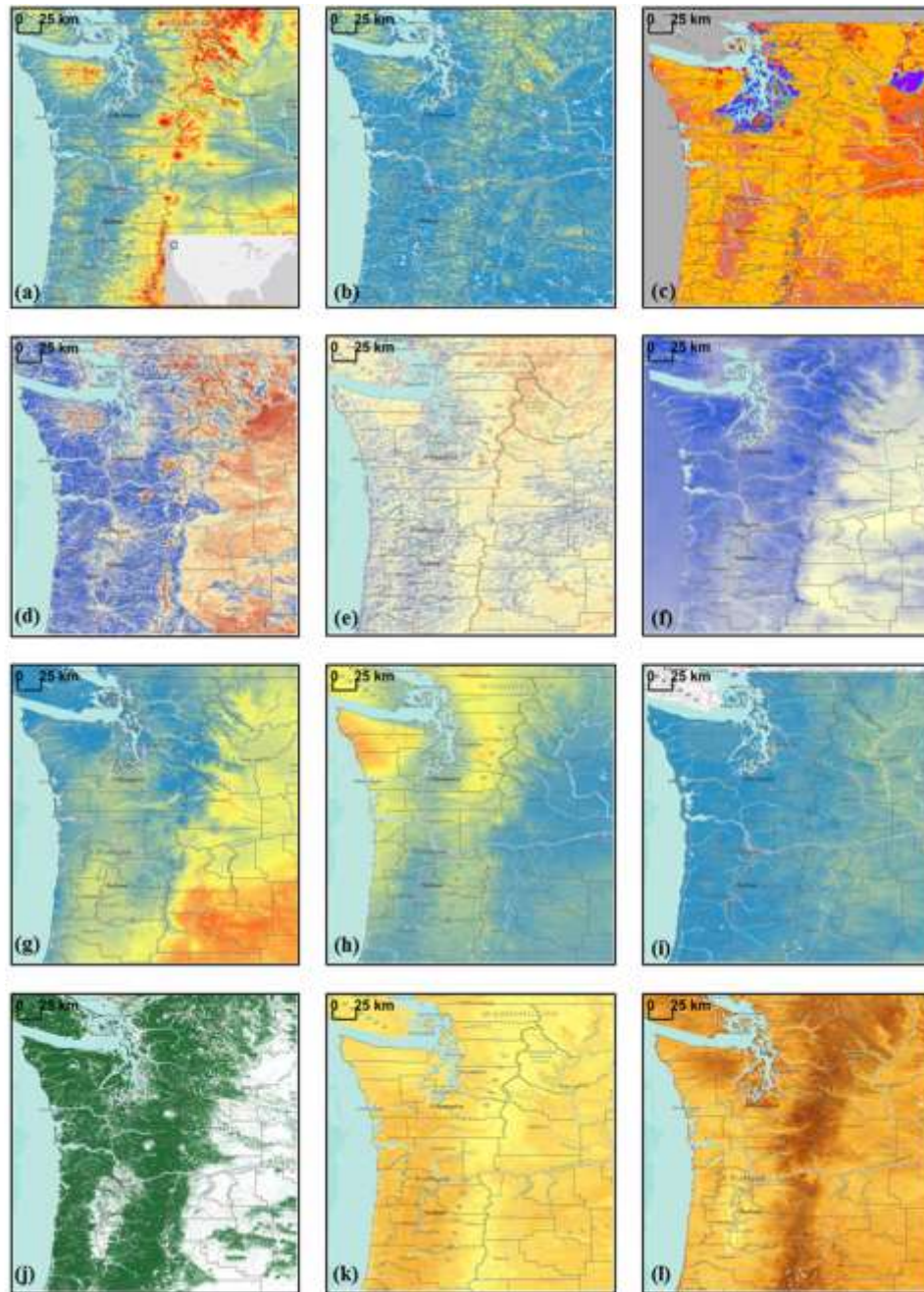


Figure 3. Examples of covariates used for the conterminous US. a) Elevation (The National Map, 2013), b) vertical distance to channel network (Conrad et al., 2015), c) SSURGO parent material (Schoeneberger et al., 2012), d) Mean monthly MODIS vegetation index for JanFeb, (LP DAAC, 2014) e) Long-term averaged mean monthly surface temperature (daytime) MODIS January (LP DAAC, 2014), f) Long term average cloud cover (Wilson and Jetz, 2016), g) Annual mean diurnal range,(O'Donnell and Ignazio, 2012) h) Total precipitation in the driest month (O'Donnell and Ignazio, 2012), i) Average vapor

pressure deficit (Daly et al., 2008), j) Tree cover (Hansen et al., 2013), k) SoilGrids250m Clay (Hengl et al., 2017), l) SoilGrids250m Sand (Hengl et al., 2017).

gSSURGO Map Unit Data

Parent material classes (87 classes) and aggregated drainage classes (4 classes) based on the representative soil components of gSSURGO map units were extracted from gSSURGO. Original parent material classes were summarized to eighty-seven distinct parent material kind classes based on Schoeneberger et al. (2012). These eighty-seven classes were nested into nine parent material kind groups based upon the geomorphic description system of The Field Book for Describing and Sampling Soils (Schoeneberger et al., 2012). This relationship is illustrated in Supplementary Table S1. For drainage classes, one limitation of the data were the local differences in methodology for mapping drainage classifications across the US. Given this limitation, the eight drainage classes extracted were reclassified to 4 drainage classes (Supplementary Table S2) to dampen the effect of inconsistent classification.

Parent material and drainage class data were missing from approximately 15% of gSSURGO map units. In order to use these covariates for spatial prediction (which requires spatially complete covariates), random forest models were built to predict the missing data using the 10 terrain attributes (see Soil Covariates) and the USGS surficial materials map (Soller et al. 2009). Parent material and drainage class prediction accuracies were 54% and 79%, respectively. These models were subsequently used to gap fill missing data from SSURGO map units. Random checks were made on predictions before maps were used as model inputs.

Accuracy Assessment

Cross-validation of soil property and class models

Ten-fold cross-validation was run to assess model accuracy for both soil property and taxonomic class models. For this validation scheme, soil samples were split into training and testing dataset. Model

training used 90% of the data, while the remaining 10% were used for model testing. Soil samples were split into training and test data such that horizon observations from a pedon were not split across training and test datasets. This 90-10 data partitioning scheme was repeated 10 times to calculate the averaged performance metrics. For each of the six numeric soil properties we derived the coefficient of determination (R^2 — the amount of variation explained by the model), mean error (ME), mean absolute error (MAE), and root mean squared error (RMSE). All equations for cross-validation metrics are provided in Supplementary materials.

Independent validation and uncertainty of soil class models

In addition to cross-validation, nine regional datasets were collated from pedon observations and used to independently validate GG and mPSC class predictions. These collated and harmonized validation datasets were collected as part of graduate student theses or as part of NRCS soil survey efforts, but which had not been included in any of the databases used in model training (Brungard et al., 2015, D’Avello and Kienast-Brown, 2016, Duniway et al., 2015, Fannesbeck, 2015, Johanson, 2016, Molstad, 2000, Stum et al., 2010). While coverage of independent data is not exhaustive due to the limited availability of soils data, these regional datasets provide an indication of modeling performance in a range of climates and landscapes across the US. Validation datasets included data from three areas in: western Utah (Beaver County, Juab County, Millard County), southeastern Utah, north-central Wyoming, southcentral New Mexico, northern Minnesota, eastern Iowa, and Maine.

Both final soil class predictions and the associated prediction probabilities were validated. Overall accuracy was used to validate soil taxonomic class prediction accuracies for the entire validation dataset, as well as for individual validation datasets. Prediction probabilities were validated using empirical uncertainty functions designed to relate the deterministic maps of GG and mPSC to independent field observations. These functions build upon methods from several prior soil class mapping studies showing positive, but non-linear trends between rates of independent observation agreement with tree-based machine learning predictions and the underlying prediction probabilities produced by these models (Nauman and Thompson, 2014; Nauman et al., 2014). This process starts by tallying instances where independent field observations are correctly and incorrectly predicted by the hardened deterministic class

maps. Then the instances are grouped by intervals of the prediction probabilities from the machine learning model associated with each field observation. The intervals were created to include approximately equal numbers of field observations using the `ggplot cut_number` function in R (Wickham, 2007). The number of intervals was initially varied in a sensitivity analysis between 10 and 20 to maintain 0.5% -1% resolution in the estimates of proportions of field observations correctly predicted – heretofore referred to as validation probabilities. We looked for trends between median prediction probabilities and validation probabilities of the intervals in the different interval binning scenarios. Based on the finding that very similar positive trends were found for all numbers of intervals tested, we looked for the best fitting regression model among all interval scenarios using a variety of empirical link functions (included linear, linear-log, quadratic, power, exponential, and generalized additive models) in R. The best models for both mPSC and GG were chosen based on the highest coefficient of determination (R^2). The fitted curves were then projected onto the mapped prediction probability surface to create a validation probability surface map. This validation probability map estimates how likely it is that the deterministic map is correct at every pixel – valuable information for end users. It also provides an idea of overall model uncertainty at a pixel because low deterministic map probabilities indicate more overall model confusion.

Results

Model Fitting

Examples of the complete coverage, gridded soil property and class maps results are illustrated in Figure 4. In this figure, examples of spatially explicit predictions of percent clay and pH are shown at 5 cm depth. The probability of occurrence of coarse loamy mPSC and Fragiudalfs across the US are also shown. The probability map of Fragiudalfs aligns with SSURGO showing the most extensive areas of occurrence of Alfisols with fragipans is the southern Mississippi valley and the southern Appalachian mountains (Bockheim and Hartemink, 2013). In addition to final reported soil property maps, the dataset collection includes preliminary maps of Mg (cmol(+)/kg), K (cmol(+)/kg), and cation exchange activity (cmol(+)/kg) that were initially tested but not validated in this study. Probability maps for each soil GG and mPSC class are also provided.

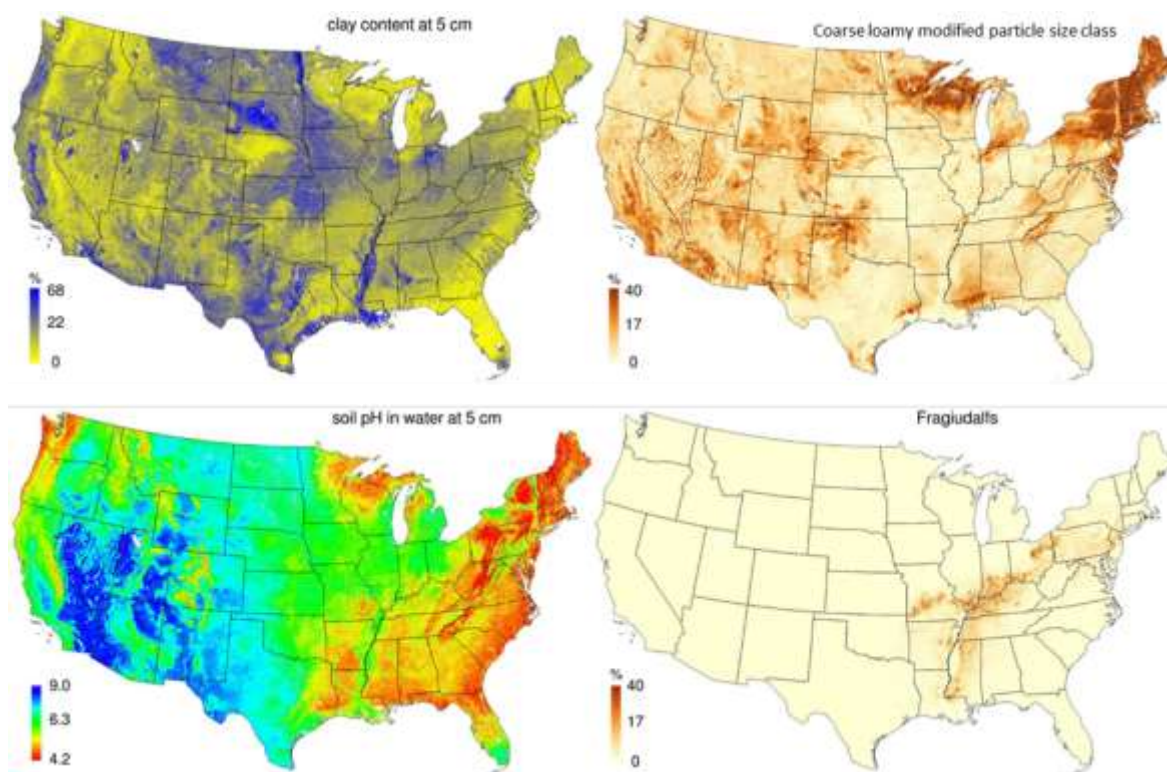


Figure 4. Examples of soil property and class maps for 2 soil properties and 2 soil classes. The complete dataset collection is available at DOI: <https://doi.org/10.18113/S1KW2H>

Summary results of the model fitting are shown in Figures 5 and 6 and Table 3. In figure 5, the variable importance (VIMP) indicates the importance of a predictor variable in a model by measuring the increase in prediction error when a predictor variable is “noised up” by randomization (Breiman, 2001). Using variable importance metrics for model interpretation can be limiting where there are groups of highly correlated variables. Strobl et al. (2008) showed correlated variables are used interchangeably in decision trees of random forest models resulting in less relevant variables receiving boosted importance. Given these concerns, we limited using the results of the VIMP analysis for model interpretation and relation to how soil survey is conducted. The top 25 predictors reported by the ranger package are shown in Figure 5. Beyond these 25 top predictors VIMP was relatively equal among the remaining predictor variables. The drop of importance of covariates is relatively gradual, which indicates that the models could not be easily reduced to <20% of the most important covariates. Depth was a strong predictor across all soil

property models indicating the strong correlation between soil properties and sample depth. Figure 5 also shows that climatic normals and bioclimatic indicators derived from PRISM were the most frequent predictor variables for both soil property and class models. DEM parameters were the second most frequent dataset, followed by SSURGO-derived and satellite data derived from MODIS and Landsat. PRISM data sets, derived from climate-elevation regressions for DEM grid cells (Daly et al., 2008), correlated more strongly overall with soil characteristics than satellite derived data, possibly because MODIS/Landsat data reflect dynamic changes in vegetation that may or may not be related to soil properties.

The frequency of DEM parameters in the top ten predictors was also in line with conventional soil survey knowledge as landscape position e.g. elevation, slope, profile curvature, is often used in soil map delineation. Both PRISM data and DEM parameters dominated the most important predictors in the soil class models, while SSURGO-derived parent material and drainage class predictor variables were present in the top 10 predictors only for soil organic C, total N, sand fraction, and clay fraction. SSURGO-derived variables were not as important for mapping great groups and mPSC classes as were climatic layers or DEM derivatives. From a practical standpoint, this result may be due to the large number of SSURGO parent material categories used which resulted in low importance per parent material category. From the perspective of soil survey, GG taxa are largely informed by climate not parent material.

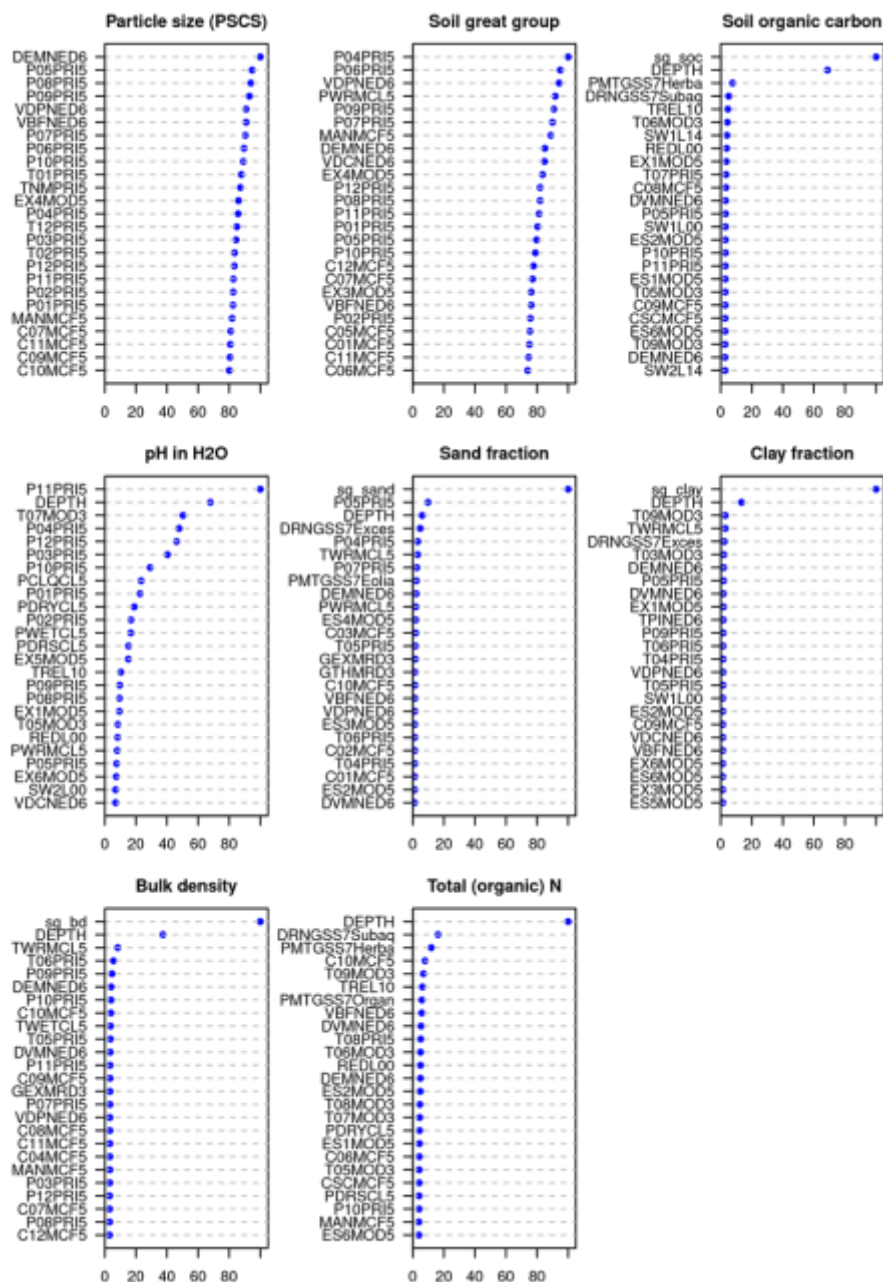


Figure 5. Variable importance (VIMP) plots per soil variable reported by the ranger package. *PRI5* indicates PRISM climatic images, *NED6* indicates DEM derivatives, *MCF* are MODIS Cloud Fraction images, *MOD3* are 1 km Land Surface Temperatures and *MOD5* are EVI images, *L14* and *L00* are the Landsat cloud-free bands, *DRNGSS* is the drainage class according to the gSSURGO, *PMTGSS* is the parent material according to the gSSURGO, *DEPTH* is the sampling (vertical) depth and *sg* are SoilGrids

datasets. Complete descriptions of codes are provided in the GitHub repository

(https://github.com/aramcharan/US_SoilGrids100m/blob/master/Covariate_Codes/SoilGrids_USA48_Covs100m.csv)

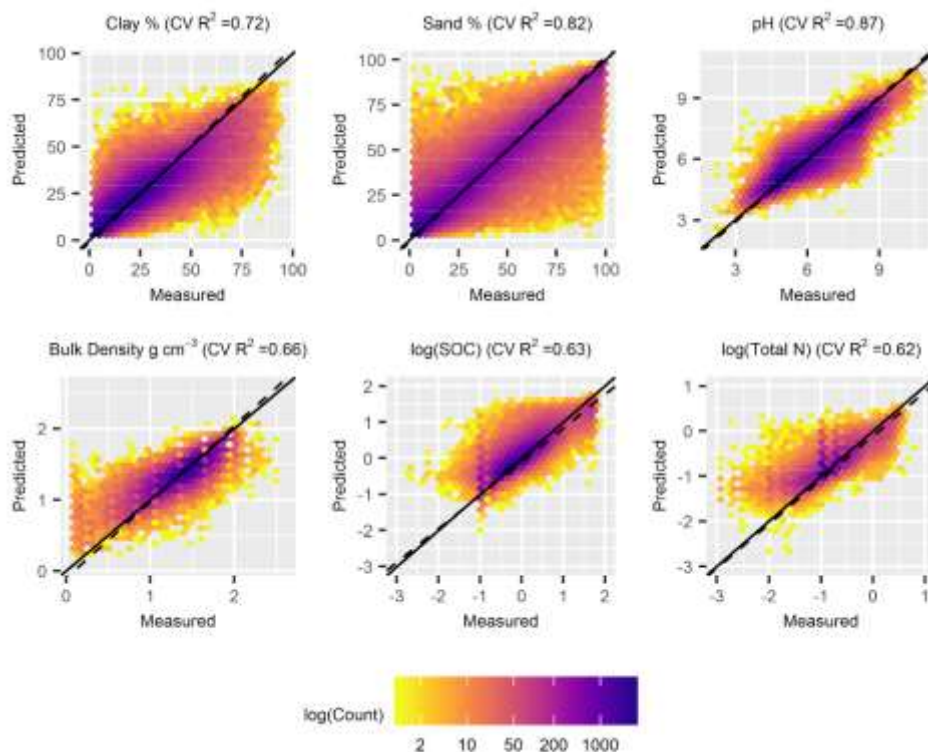


Figure 6. Correlation plots, based on cross-validation results, for each soil property with the line of perfect fit (solid line) and the line of best fit (least squared method) (dashed line).

Accuracy Assessment

Cross-validation of soil property and class models

Ten-fold cross-validation was used to calculate the performance metrics of the models for soil properties and classes. We note that given the spatial clustering of the soil samples e.g. high sampling density on

agricultural land and low sampling density in national forests, it is likely the validation results are optimistic and we must assume there is spatial autocorrelation of prediction errors. More robust validation results can likely be achieved with a testing dataset collected following a validation strategy such as an objective probability sampling (Brus et al. 2015). The average coefficient of determination (R-square) (Eqn.S2) for soil property models was 0.72 (Table 3), with a low of 0.62 for total N and high of 0.87 for pH. For the soil class models, cross-validation resulted in an average misclassification rate of 0.34 for the mPSC model and 0.40 for the Soil GG model, hence a mapping accuracy of 66% and 60% respectively. We provide only mapping accuracy statistics and not for example the Kappa statistics as these have shown not to be as useful for interpretation and comparison of classification accuracy (Pontius and Millones, 2011). Soil property models underestimated values as indicated by Mean Error (ME) in Table 3. Figure 6 shows the correlation plots for soil properties along with the line of perfect fit (solid line) and the line of best fit (least square method) (dashed line). Based on these correlation plots, clay, sand, and pH predictions were close to measured values over the range of soil property values. Bulk density and SOC showed an overestimation for low values and underestimation of high values while total N showed a consistent underestimation across the range of values (0.001 – 5.5 wt%). Figure 7 shows a comparison of the soil property spatial prediction results with SoilWeb (Beaudette and O'Geen, 2009), the online soil survey for California based on SSURGO and STATSGO, for three soil properties - percent clay, bulk density, and pH. Visual inspection of the maps derived from completely different modeling approaches show similar spatial patterns. The resolution of the spatial prediction results are higher (100 m compared to 1 km) but the comparison shows our results underestimated values in the high range for given soil properties, compared to SoilWeb (in line with the results of the performance metrics and correlation plots).

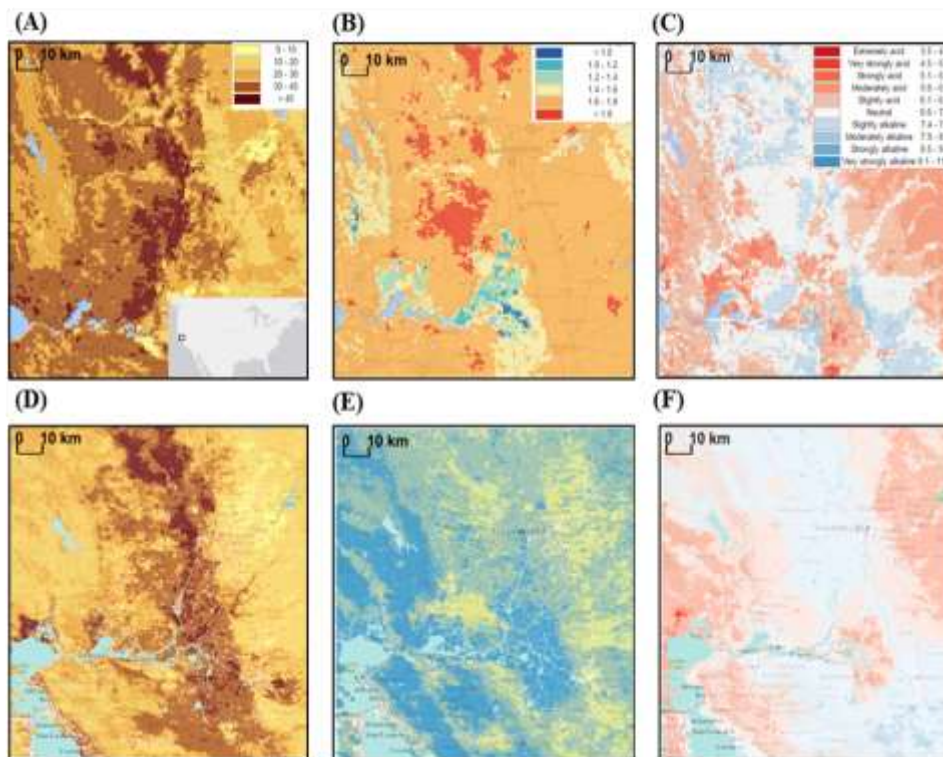


Figure 7. Comparison of SoilWeb Soil Properties (Beaudette and O'Geen, 2009) (top row) near Sacramento, CA (inset of a) with US48 SoilGrids100m+ results (bottom row). a) and d) Percent clay, wt %, b) and e) Bulk density g cm^{-3} , c) and f) pH. Legends are the same for both data sources. SoilWeb properties are derived from SSURGO and STATSGO.

Independent data validation of soil class model

The overall accuracy of GG predictions using all independent validation observations was 37%. The overall mPSC accuracy using all independent validation observations was 42%. Validation of GG and mPSC predictions for each independent dataset are presented in Figures 8 and 9. Great group prediction accuracy ranged between 24% and 58%. Modified particle size class prediction accuracy ranged between 24% and 93%.

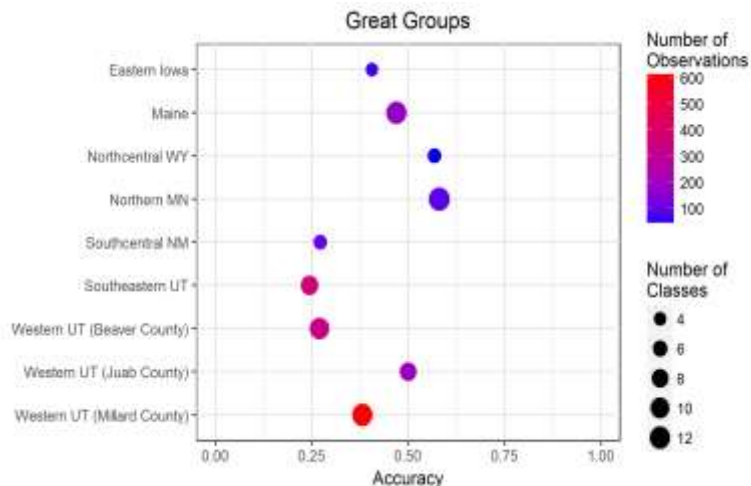


Figure 8. Great Group prediction accuracy by independent validation dataset. Number of observations is the number of great group observations in each validation dataset. Number of classes is the number of great group classes in each validation dataset.

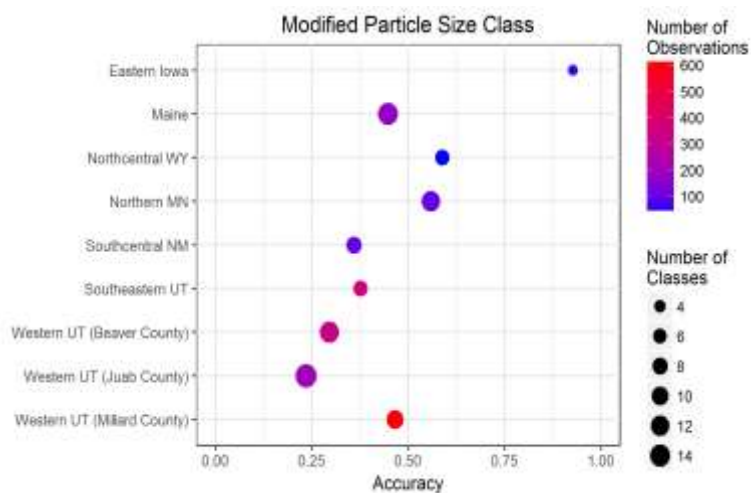


Figure 9. Modified particle size class prediction accuracy by independent validation dataset. Number of observations is the number of modified particle size class observations in each validation dataset. Number of classes is the number of modified particle size classes in each validation dataset.

Empirical Uncertainty of Soil Classes

Relationships between the ensemble model prediction probabilities and validation probabilities were quite strong. Linear-log functions with 10 probability intervals fit the GG data best (Figure 10A) while 12 intervals resulted in the best mPSC fit (Figure 10B). Strong linear-log relationships for both probability distributions support the hypothesis that the deterministic probabilities produced by random forest models hold valuable information about uncertainty in final predictions, but that the relationship to prediction uncertainty is non-linear. Overall, mPSC had higher validation probabilities reflecting the higher overall accuracy statistics. Relatively similar spatial patterns in validation probabilities can be seen in comparing the GG (Figure 10C) and mPSC (Figure 10D). Both show better accuracies in the central mid-western states (NE, MI, IA, IL), portions of Texas, and along the eastern coastal plain, likely due to the higher density of soil samples in these areas.

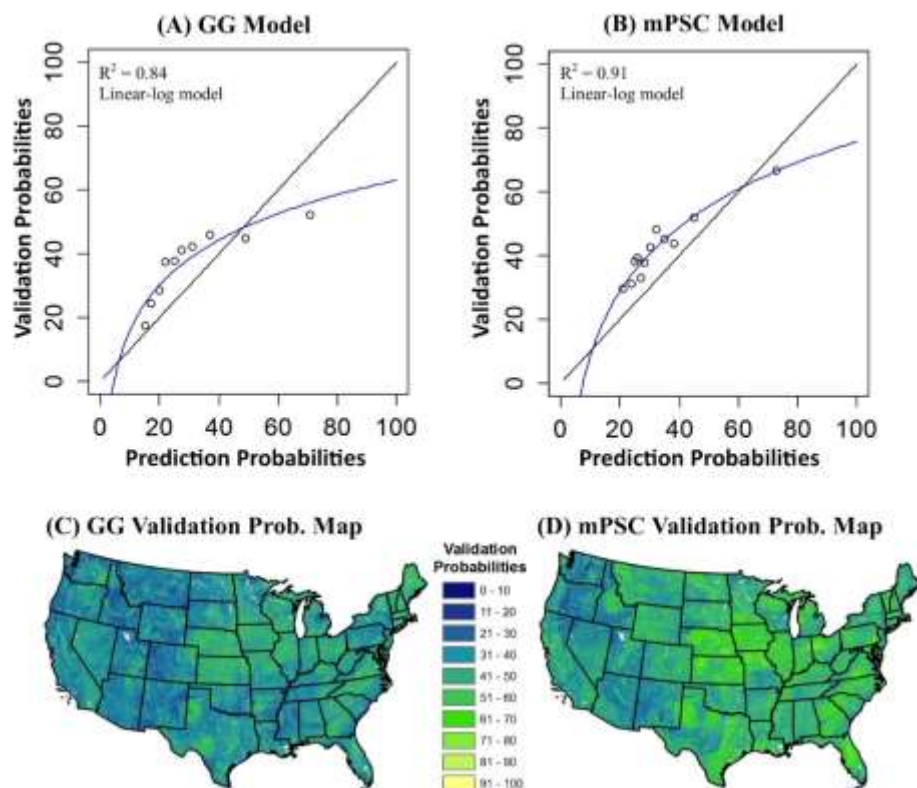


Figure 10. Empirical uncertainty analyses results. a) Empirical relationships between prediction and validation probabilities for Great Groups, b) and modified Particle Size Classes, along with c) resulting

maps for great groups, and d) modified particle size classes. Graphs a) and b) include a 1:1 reference line (black).

Discussion

Machine Learning and Soil Science

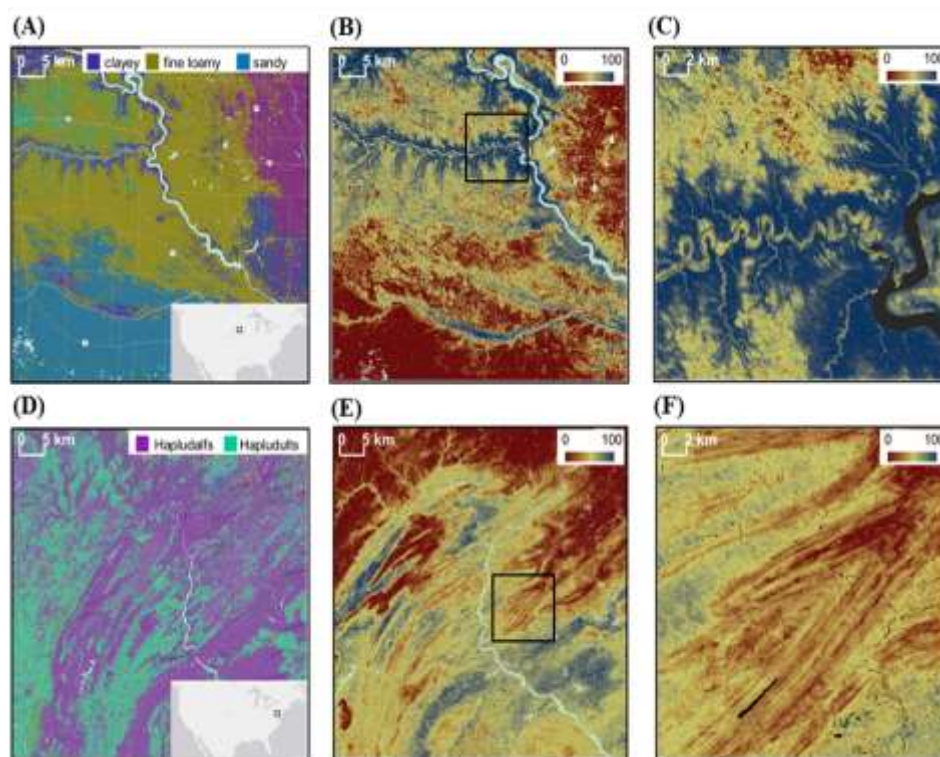


Figure 11. Hardened and probability soil class map results. a, Map of mPSC near Pierre, SD (US map inset). b, Probability map of clayey soil. c, Probability map of clayey soil zoomed in. d, Map of GG near Harrisburg, PA (US map inset). e) Probability map of Hapludalfs. f) Probability map of Hapludalfs zoomed in.

This study harnessed the capabilities of a high-performance computing environment along with parallel programmed machine learning algorithms to create soil property and class maps with exhaustive

coverage for the conterminous US; illustrated in Figures 4, 7, and 11, respectively. We worked within a relatively new scientific paradigm where large datasets from a variety of sources were integrated with quantitative methods to increase the value of conventional datasets. To illustrate our point, we present a SSURGO map unit in Utah, USA where seven soil types are aggregated in a SSURGO association map unit (Figure 12). This variation of soil components within map units can limit the usefulness of soils maps for land managers. Previous research shows that this map unit has been implicated as a dust emissions source possibly causing accidents on Interstate 70 (freeway) because of heavy grazing and highly erodible soils (Flagg et al., 2014). However, in order to manage for that, the variability in soil texture within this map unit is very important. In this case, dominant southwest winds blowing saltating sands from the southwest onto clayey soils derived from Mancos shales is a likely mechanism for dust mobilization (Miller et al., 2012; Lu and Shao, 1999). Therefore, a manager might want to initially focus on stabilizing the sandier areas upwind so they don't bombard the finer areas with saltating sands. However, this solution might not occur to a manager without the spatial context of SoilGrids100m+' finer resolution.

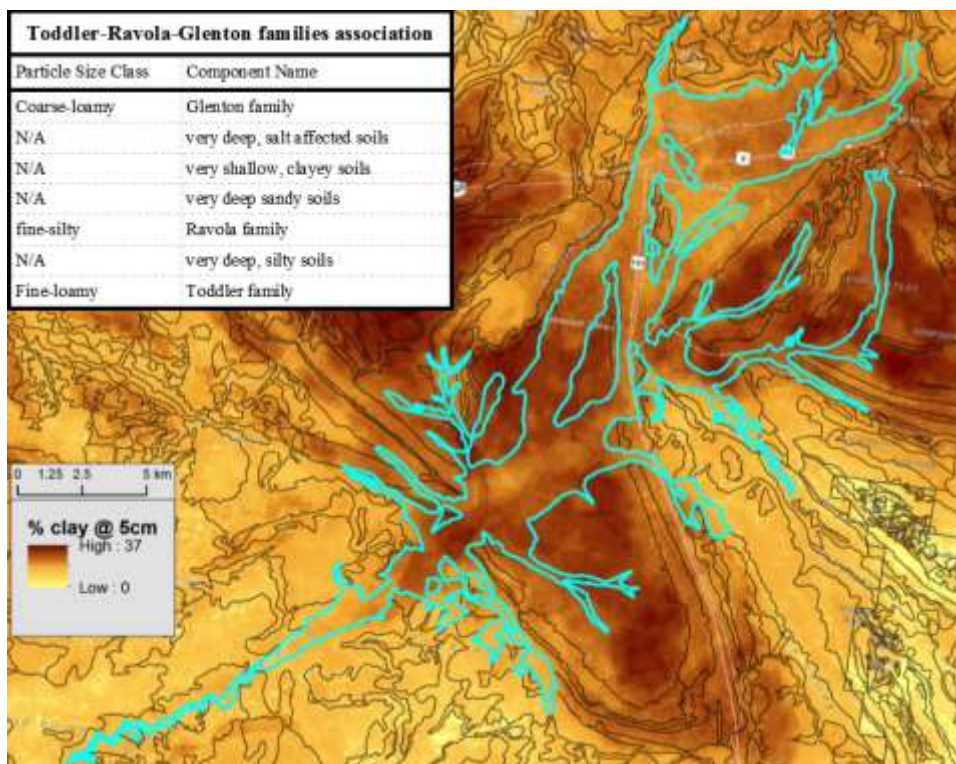


Figure 12. The Ten-Mile Canyon region near Moab, UT was mapped with large association map units that often aggregate soils with widely varying management strategies associated with dust emission. This

map shows that in terms of near surface clay content variation and variable attribution of SSURGO map unit component.

Our results were made possible through collaboration with soil and computer scientists, ensuring expert knowledge was captured and used to validate results. The collaboration with soil scientists within government agencies and land grant universities enabled us to make many decisions on how to prepare the data, run the analyses, evaluate errors and inconsistencies in the map products, conduct visual and quantitative validations of results, and inform future research efforts within this domain. With awareness of the “data deluge” in many sciences (Roudier et al., 2015), we developed our analysis in an open science framework, providing the necessary metadata, data and code in an open access Github repository (https://github.com/aramcharan/US_SoilGrids100m).

Limitations of working with conventional soil data

Our work attempted to address some of the main challenges of working with conventional soils datasets. These include working with map units comprising multiple soil components, managing missing data, identifying taxonomic classifications from multiple editions of US *Soil Taxonomy*, and assessing the accuracy of soil maps when independent data are limited. Our approach to these challenges are discussed below.

Currently, the SSURGO database represents soil variability at scales within individual map unit polygons by assigning composition (or proportion) of multiple SSURGO components, as well as inclusions of minor soil components and non-soil areas to map unit identifiers (Nauman and Thompson, 2014). Previous research has worked to disaggregate map units with soil-landscape models, (Bui and Moran, 2001; de Bruin et al., 1999; Wielemaker et al., 2001). Chaney et al. (2016) provides an example of this for the conterminous US. In order to exploit information represented in the SSURGO database, we applied previous research that assembled soil parent material classes, based on the representative component percentage for SSURGO, to create a parent material conterminous map (Schoeneberger et al., 2012). The tradeoff in selecting a representative soil component for a map unit was the loss of information

contained within the map unit pertaining to additional soil components. We also did not have the actual location of components within the map unit, which would have a varying effect on models as the number of components changed and the size of the map unit changed.

Another limitation of working with conventional soil data was the classification of GG data using multiple editions of US *Soil Taxonomy*. Of the 328,380 observations of most recent GG extracted from the NASIS database, 6,622 (2%) had obsolete classifications according to the 12th edition of US *Soil Taxonomy* (Soil Survey Staff, 2014). In order to make the most of conventional soil data, future work could include re-correlating obsolete data. With multiple editions of great group classes in the training data, there is the potential for confusion between overlapping taxonomic concepts which could reduce the model accuracy. If model accuracy is high, the confusion matrix results for the GG model could inform strategies to re-correlate obsolete classes by providing insight into which GG classes misclassify with each other.

Overall accuracy metrics for the soil taxonomic class models were acceptable considering the geographic extent of the model. However, differences in validation accuracy between independent validation datasets indicates spatially variable prediction accuracy. The lack of a clear trend between the number of observations, the number of classes, observation density (Tables 1 and 2) and prediction accuracy (Figures 8 and 9) indicates that differences in validation accuracy between areas is not because of differences in the independent validation data. It is difficult to exactly specify what conditions caused the variability in accuracy metrics between independent validation datasets. However, it is likely that this variability is a result of several factors including the frequency distribution of observed soil taxonomic classes (Brungard et al., 2015) and similarity between taxonomic classes (Rossiter et al., 2017).

Differences in prediction accuracy between areas are also likely a result of differences in the strength of covariate-class relationships. Further improvement in predictive accuracy will likely result from model stratification, the addition of regionally-important covariates e.g. soil erosion/disturbance rates, management practices such as irrigation, and the inclusion of additional training observations at locations of low prediction quality. Variability in accuracy metrics (and thus variability in prediction quality) likely also results from a mismatch between grid size predictions (100 m) and the inherent scale at which taxonomic classes vary across different landscapes. In our visual review of the predictions (data not shown) it

appeared that for some landscapes, 100 m was too coarse to capture the geographic scale of soil GG taxonomic variability. Using eastern Iowa as an example, the number of GG occurring at fine scales depends on the landscape and the proximity of soil features to taxonomic breaks. In this case, there are three geologic strata exposed through erosion with different mineralogies and erosion histories. These pedons also straddle taxonomic breaks with diagnostic horizons and soil features found in multiple taxa without large differences in properties. This highlights the difficulties in predicting taxonomic classes when the similarities between taxa are not consistent between higher taxa and across soil landscapes. It is possible that soil taxonomic class predictions could improve if environmental covariates at resolutions < 100 m were used for modeling (e.g. Nauman & Duniway, 2016); however, this would increase computation complexity for a model of this large an extent and limit the number of usable covariates e.g. PRISM data should not be downscaled to 30m where microclimate effects increase in importance.

Empirical uncertainty functions were created for soil class maps to compare deterministic maps of GG and mPSC to the independent validation data. The empirical uncertainty function predicted validation probabilities that represent estimates of the independent validation data match rates that are more realistic representations of local model uncertainty at each pixel. With the high R-square values for the models to rescale prediction probabilities (84% and 91% for GG and mPSC respectively), the uncertainty analyses suggest the probabilities produced by the models are informative even though they were lower than expected. The disadvantage of these analyses is the deterministic maps used to validate independent observations only use the top predicted class (Top-1 prediction), reducing the output of the models from a distribution of soil class probabilities to one predicted class. For soil class data with many classes and/or class boundaries that are abstract or overlap conceptually, there would be a considerable loss of information and a perceived low model performance. This is evident in comparing the results for the validation probabilities for the two soil classes mapped. With more soil GG classes (291 classes), the validation probabilities were lower than the mPSC classes (78 classes). Future work can repeat the uncertainty analyses with the top 5 predicted classes, as is often reported in the machine learning literature (Szegedy et al., 2016). Alternatively, we can compare results with another product at similar scale (gSSURGO or STATSGO).

The results of the soil class models demonstrate the challenges of working with conventional soil concepts. Our results show that there are categories within US *Soil Taxonomy* that can take advantage of soil mapping concepts without much revision by soil science experts (mPSC), while other categories require extensive input by experts to update conventional soil data to apply these methods (GG). Modifications of USDA particle size classes similar to what we mapped (mPSC) have proved to be useful for regional scale land management (Nauman and Duniway, 2016; Nauman et al., 2017) and our results support further development.

Conclusion

This work demonstrated the use of a high-performance computing environment and ensemble machine learning methods to produce gridded soil property and class maps for the conterminous US at 100 meters. The results of this study provide documented estimates and uncertainties of machine learning predictions, given current available national soils and environmental datasets, of six soil properties (percent organic C, total N, bulk density, pH, percent sand, and clay) at seven standard depths (0, 5, 15, 30, 60, 100, 200 cm), and two soil classification schemes (GG and mPSC). By implementing the study within an automated framework, gridded maps with exhaustive coverage can be rapidly improved (less than 1 week of computing) and shared as more data becomes available and more users test these data products.

The average R-square for soil property models was 0.72, while soil class models had an average 63% classification accuracy. Independent data was additionally used to validate soil class model predictions (1,999 points for GG and 2,012 points for mPSC) and conduct empirical uncertainty analyses. Nine regional datasets were used to validate soil class maps and while we acknowledge an evaluation was not conducted for the conterminous US, we consider the test case areas a step forward in the process.

This collaborative study extended the current soils data resources for the US to meet the needs of geographic simulation models dependent on spatially explicit, three-dimensional reference soil geographic datasets by creating a product that is easier to integrate with models compared to multi-component map units. Even though mapping accuracy is variable and likely lower than gSSURGO in

some areas, the soil property maps can immediately be used for refinement/testing of human landscape models and used by land managers who require spatial variability of soil characteristics within SSURGO map units . The data, metadata, covariates, models, and codes can be freely accessed via DOI:

<https://doi.org/10.18113/S1KW2H> as well as a public Github repository

(https://github.com/aramcharan/US_SoilGrids100m).

References

1. Amundson, R., Berhe, A.A., Hopmans, J.W., Olson, C., Sztein, A.E. and Sparks, D.L., 2015. Soil and human security in the 21st century. *Science*, 348(6235), p.1261071.
2. Arrouays, D., Grundy, M.G., Hartemink, A.E., Hempel, J.W., Heuvelink, G.B., Hong, S.Y., Lagacherie, P., Lelyk, G., McBratney, A.B., McKenzie, N.J. and dL Mendonca-Santos, M., 2014. Chapter Three-GlobalSoilMap: Toward a fine-resolution global grid of soil properties. *Advances in agronomy*, 125, pp.93-134.
3. Batjes, N.H., 2016. Harmonized soil property values for broad-scale modelling (WISE30sec) with estimates of global soil carbon stocks. *Geoderma*, 269, pp.61-68.
4. Beaudette, D. E., & O'Geen, A. T. (2009). Soil-Web: an online soil survey for California, Arizona, and Nevada. *Computers & Geosciences*, 35(10), 2119-2128.
5. Brady, N.C. and Weil, R.R., 2008. An introduction to the nature and properties of soils. *Prentice Hall, Upper Saddle River, NJ*.
6. Breiman, L., 2001. Random forests. *Machine learning*, 45(1), pp.5-32.
7. Brungard, C. W., Boettinger, J. L., Duniway, M. C., Wills, S. A., & Edwards Jr., T. C. (2015). Machine learning for predicting soil classes in three semi-arid landscapes. *Geoderma*, 239–240, 68–83. <https://doi.org/10.1016/j.geoderma.2014.09.019>
8. Brus, D.J., Kempen, B. and Heuvelink, G.B.M., 2011. Sampling for validation of digital soil maps. *European Journal of Soil Science*, 62(3), pp.394-407.

9. Bockheim, J.G. and Hartemink, A.E., 2013. Soils with fragipans in the USA. *Catena*, 104, pp.233-242.
10. Bui, E.N., 2016. Data-driven Critical Zone science: A new paradigm. *Science of The Total Environment*.
11. Bui, E.N., Moran, C.J., 2001. Disaggregation of polygons of surficial geology and soil maps using spatial modelling and legacy data. *Geoderma* 103 (1–2), 79–94.
12. Bui, E.N., Loughhead, A. and Corner, R., 1999 Extracting soil-landscape rules from previous soil surveys Aust J Soil Res 37 495-508 .
13. Caudle, D., H. Sanchez, J. DiBenedetto, C. Talbot, and M. Karl. 2013. Interagency ecological site handbook for rangelands. USDA-NRCS, USDA-FS, and Dep. of Interior–Bureau of Land Management, Washington, DC. <http://jornada.nmsu.edu/sites/jornada.nmsu.edu/files/InteragencyEcolSiteHandbook.pdf> (verified 7 Sept. 2016)
14. Chaney, N.W., Wood, E.F., McBratney, A.B., Hempel, J.W., Nauman, T.W., Brungard, C.W. and Odgers, N.P., 2016. POLARIS: A 30-meter probabilistic soil series map of the contiguous United States. *Geoderma*, 274, pp.54-67.
15. Chen, T. and Guestrin, C., 2016, August. Xgboost: A scalable tree boosting system. In Proceedings of the 22Nd ACM SIGKDD International Conference on Knowledge Discovery and Data Mining (pp. 785-794). ACM.
16. Conrad, O., Bechtel, B., Bock, M., Dietrich, H., Fischer, E., Gerlitz, L., ... & Böhner, J. (2015). System for automated geoscientific analyses (SAGA) v. 2.1. 4. *Geoscientific Model Development*, 8(7), 1991-2007.
17. Cutler, D.R., Edwards, T.C., Beard, K.H., Cutler, A., Hess, K.T., Gibson, J. and Lawler, J.J., 2007. Random forests for classification in ecology. *Ecology*, 88(11), pp.2783-2792.

18. Daly, C., Halbleib, M., Smith, J.I., Gibson, W.P., Doggett, M.K., Taylor, G.H., Curtis, J. and Pasteris, P.P., 2008. Physiographically sensitive mapping of climatological temperature and precipitation across the conterminous United States. *International journal of climatology*, 28(15), pp.2031-2064.
19. D'avello, T., Kienast-Brown, S. 2016. [Boundary Waters Canoe Wilderness Area Soil Survey]. Unpublished raw data.
20. de Bruin, S., Wielemaker, W.G., Molenaar, M., 1999. Formalisation of soil–landscape knowledge through interactive hierarchical disaggregation. *Geoderma* 91 (1–2), 151–172.
21. Dietterich, T.G., 2000, June. Ensemble methods in machine learning. In *International workshop on multiple classifier systems* (pp. 1-15). Springer Berlin Heidelberg.
22. Duniway, M.C., B.T. Bestelmeyer, and A. Tugel. 2010. Soil processes and properties that distinguish ecological sites and states. *Rangelands* 32:9–15. doi:10.2111/Rangelands-D-10-00090.1
23. Duniway, M.C., Brungard, C.W., Darger, A., Schupp, E., Boettinger, J.L. 2015. [Data collection to support Sagebrush Management]. Unpublished raw data.
24. Duval, J.S., Carson, J.M., Holman, P.B., and Darnley, A.G., 2005, Terrestrial radioactivity and gamma-ray exposure in the United States and Canada: U.S. Geological Survey Open-File Report 2005-1413. <https://mrdata.usgs.gov/radiometric/> accessed 01/05/2017.
25. Fire Sciences Laboratory, Rocky Mountain Research. Historical Natural Fire Regimes, Version 2000. Fire Sciences Laboratory, Rocky Mountain Research, Missoula, Montana.
26. Folberth, C., Skalský, R., Moltchanova, E., Balkovič, J., Azevedo, L.B., Obersteiner, M. and Van Der Velde, M., 2016. Uncertainty in soil data can outweigh climate impact signals in global crop yield simulations. *Nature Communications*, 7.

27. Friedman, J., Hastie, T. and Tibshirani, R., 2001. *The elements of statistical learning* (Vol. 1). Springer, Berlin: Springer series in statistics.
28. Friedman, J.H., 2002. Stochastic gradient boosting. *Computational Statistics & Data Analysis*, 38(4), pp.367-378.
29. Fannesbeck, B.B. 2015. Digital Soil Mapping Using Landscape Stratification for Arid Rangelands in the Eastern Great Basin , Central Utah. All Grad. Theses Diss. Paper 4525, Utah State University, Logan.
30. Grimm, R., Behrens, T., Märker, M. and Elsenbeer, H., 2008. Soil organic carbon concentrations and stocks on Barro Colorado Island—digital soil mapping using Random Forests analysis. *Geoderma*, 146(1), pp.102-113.
31. Wickham, H. and Wickham, M.H., 2007. The ggplot package.
32. Hansen, M. C., P. V. Potapov, R. Moore, M. Hancher, S. A. Turubanova, A. Tyukavina, D. Thau, S. V. Stehman, S. J. Goetz, T. R. Loveland, A. Kommareddy, A. Egorov, L. Chini, C. O. Justice, and J. R. G. Townshend. 2013. “High-Resolution Global Maps of 21st-Century Forest Cover Change.” *Science* 342 (15 November): 850–53. Data available online from: <http://earthenginepartners.appspot.com/science-2013-global-forest>.
33. Helmick, J.L., Nauman, T.W. and Thompson, J.A., 2013. Developing and assessing prediction intervals for soil property maps derived from legacy databases. *In GlobalSoilMap Proceedings Orlean, France Arrouays et al.,(eds)*.
34. Henderson, B.L., Bui, E.N., Moran, C.J. and Simon, D.A.P., 2005. Australia-wide predictions of soil properties using decision trees. *Geoderma*, 124(3), pp.383-398.
35. Hengl, T., de Jesus, J.M., Heuvelink, G.B., Gonzalez, M.R., Kilibarda, M., Blagotić, A., Shangquan, W., Wright, M.N., Geng, X., Bauer-Marschallinger, B. and Guevara, M.A., 2017. SoilGrids250m: Global gridded soil information based on machine learning. *PLoS one*, 12(2), p.e0169748.

36. Hengl, T., de Jesus, J.M., MacMillan, R.A., Batjes, N.H., Heuvelink, G.B., Ribeiro, E., Samuel-Rosa, A., Kempen, B., Leenaars, J.G., Walsh, M.G. and Gonzalez, M.R., 2014. SoilGrids1km—global soil information based on automated mapping. *PLoS One*, 9(8), p.e105992.
37. Hengl, T., Heuvelink, G.B., Kempen, B., Leenaars, J.G., Walsh, M.G., Shepherd, K.D., Sila, A., MacMillan, R.A., de Jesus, J.M., Tamene, L. and Tondoh, J.E., 2015. Mapping soil properties of Africa at 250 m resolution: Random forests significantly improve current predictions. *PloS one*, 10(6), p.e0125814.
38. Hengl T, Mendes de Jesus J, Heuvelink GBM, Ruiperez Gonzalez M, Kilibarda M, Blagotić A, et al. (2017) SoilGrids250m: Global gridded soil information based on machine learning. *PLoS ONE* 12(2): e0169748.
39. Hudson, B.D., 1992. The soil survey as paradigm-based science. *Soil Science Society of America Journal*, 56(3), pp.836-841.
40. Ishwaran, H. and Kogalur, U., 2013. Random forests for survival, regression and classification (RF-SRC). URL <http://cran.r-project.org/web/packages/randomForestSRC/>. R package version, 1.
41. Jenny, H., 1994. *Factors of soil formation: a system of quantitative pedology*. Courier Corporation.
42. Jenny, H. and Leonard, C.D., 1934. Functional relationships between soil properties and rainfall. *Soil Science*, 38(5), pp.363-382.
43. Johanson, J. 2016. Ecological Site Development Data for Maine. Unpublished raw data.
44. Jones, J.W., Antle, J.M., Basso, B., Boote, K.J., Conant, R.T., Foster, I., Godfray, H.C.J., Herrero, M., Howitt, R.E., Janssen, S. and Keating, B.A., 2016. Brief history of agricultural systems modeling. *Agricultural Systems*.

45. Kheir, R.B., Greve, M.H., Bøcher, P.K., Greve, M.B., Larsen, R. and McCloy, K., 2010. Predictive mapping of soil organic carbon in wet cultivated lands using classification-tree based models: The case study of Denmark. *Journal of Environmental Management*, 91(5), pp.1150-1160.
46. Kuhn, M. 2008. Building Predictive Models in R Using the caret Package. *Journal of Statistical Software*, 28(i05).
47. Kuhn, M. and Johnson, K., 2013. *Applied predictive modeling* (pp. 389-400). New York: Springer.
48. Kuchler, A.W. 1964. Potential Natural Vegetation of the Conterminous United States. American Geographical Society, Special Publication No. 36.
49. Lacoste, M., Mulder, V.L., Richer-de-Forges, A.C., Martin, M.P. and Arrouays, D., 2016. Evaluating large-extent spatial modeling approaches: A case study for soil depth for France. *Geoderma Regional*, 7(2), pp.137-152.
50. Latinne, P., Debeir, O. and Decaestecker, C., 2001, July. Limiting the number of trees in random forests. In *International Workshop on Multiple Classifier Systems* (pp. 178-187). Springer Berlin Heidelberg.
51. Manzoni, S. and Porporato, A., 2009. Soil carbon and nitrogen mineralization: theory and models across scales. *Soil Biology and Biochemistry*, 41(7), pp.1355-1379.
52. McKenzie, N.J. and Ryan, P.J., 1999. Spatial prediction of soil properties using environmental correlation. *Geoderma*, 89(1), pp.67-94.
53. Moran, C.J. and Bui, E.N., 2002. Spatial data mining for enhanced soil map modelling. *International Journal of Geographical Information Science*, 16(6), pp.533-549.
54. Molstad, N. E. 2000. Landscapes, soil morphology and switchgrass management and productivity in the Chariton River Valley, Iowa. Unpubl. Diss. MS thesis, Iowa State University, Ames.

55. Mulder V, Lacoste M, Richer-de Forges A, Martin M, Arrouays D. National versus global modelling the 3D distribution of soil organic carbon in mainland France. *Geoderma*. 2016;263:16–34.
56. National Academy of Sciences. 2001. Grand challenges in environmental sciences. Natl. Acad. Press, Washington, DC.
57. National Academy of Sciences. 2010. Landscapes on the edge: New horizons for research on Earth's surface. Natl. Acad. Press, Washington, DC.
58. Nauman, T.W. and Duniway, M.C., 2016. The Automated Reference Toolset: A Soil-Geomorphic Ecological Potential Matching Algorithm. *Soil Science Society of America Journal*, 80(5), pp.1317-1328.
59. Nauman, T.W., Duniway, M.C., Villarreal, M.L., & Poitras, T.B. 2017. Disturbance automated reference toolset (DART): Assessing patterns in ecological recovery from energy development on the Colorado Plateau. *Science of The Total Environment*
60. Nauman, T. W., and J. A. Thompson. 2014. Semi-automated disaggregation of conventional soil maps using knowledge driven data mining and classification trees. *Geoderma* 213:385-399.
61. Nauman, T.W., Thompson, J.A., & Rasmussen, C. (2014). Semi-Automated Disaggregation of a Conventional Soil Map Using Knowledge Driven Data Mining and Random Forests in the Sonoran Desert, USA. *Photogrammetric Engineering & Remote Sensing*, 80, 353-366
62. NCSS (2015), National Cooperative Soil Characterization Database, National Cooperative Soil Survey, Lincoln, NE. <http://ncsslabsdatamart.sc.egov.usda.gov/>, accessed 08/12/2015.
63. Odeh, I.O.A., McBratney, A.B. and Chittleborough, D.J., 1994. Spatial prediction of soil properties from landform attributes derived from a digital elevation model. *Geoderma*, 63(3), pp.197-214.

64. Odgers, N.P., Libohova, Z. and Thompson, J.A., 2012. Equal-area spline functions applied to a legacy soil database to create weighted-means maps of soil organic carbon at a continental scale. *Geoderma*, 189, pp.153-163.
65. O'Donnell, M.S. and Ignizio, D.A., 2012. Bioclimatic predictors for supporting ecological applications in the conterminous United States. *US Geological Survey Data Series*, 691(10).
66. Odgers, N.P., Libohova, Z. and Thompson, J.A., 2012. Equal-area spline functions applied to a legacy soil database to create weighted-means maps of soil organic carbon at a continental scale. *Geoderma*, 189, pp.153-163.
67. Oshiro, T.M., Perez, P.S. and Baranauskas, J.A., 2012, July. How many trees in a random forest?. In International Workshop on Machine Learning and Data Mining in Pattern Recognition (pp. 154-168). Springer Berlin Heidelberg.
68. Pachepsky, Y.A., Timlin, D.J. and Rawls, W.J., 2001. Soil water retention as related to topographic variables. *Soil Science Society of America Journal*, 65(6), pp.1787-1795.
69. Park, S.J. and Vlek, P.L.G., 2002. Environmental correlation of three-dimensional soil spatial variability: a comparison of three adaptive techniques. *Geoderma*, 109(1), pp.117-140.
70. Pekel, J.F., Cottam, A., Gorelick, N. and Belward, A.S., 2016. High-resolution mapping of global surface water and its long-term changes. *Nature*.
71. Pontius Jr, R.G. and Millones, M., 2011. Death to Kappa: birth of quantity disagreement and allocation disagreement for accuracy assessment. *International Journal of Remote Sensing*, 32(15), pp.4407-4429.
72. R Core Team (2016). R: A language and environment for statistical computing. R Foundation for Statistical Computing, Vienna, Austria. URL <http://www.R-project.org/>.

73. Rossiter, D.G., Zeng, R., Zhang, G.L. 2017. Accounting for taxonomic distance in accuracy assessment of soil class predictions. *Geoderma*, 292, pp. 118-127. DOI: 10.1016/j.geoderma.2017.01.012
74. Roudier, P., Ritchie, A., Hedley, C. and Medyckyj-Scott, D., 2015. The rise of information science: a changing landscape for soil science. In *IOP Conference Series: Earth and Environmental Science* (Vol. 25, No. 1, p. 012023). IOP Publishing.
75. Sanchez, P.A., Ahamed, S., Carré, F., Hartemink, A.E., Hempel, J., Huising, J., Lagacherie, P., McBratney, A.B., McKenzie, N.J., de Lourdes Mendonça-Santos, M. and Minasny, B., 2009. Digital soil map of the world. *Science*, 325(5941), pp.680-681.
76. Schoeneberger, P.J., D.A. Wysocki, E.C. Benham, and Soil Survey Staff. 2012. Field book for describing and sampling soils, Version 3.0. Natural Resources Conservation Service, National Soil Survey Center, Lincoln, NE.
77. Soil Survey Staff. 2016. Gridded Soil Survey Geographic (gSSURGO) Database for the Conterminous United States. United States Department of Agriculture, Natural Resources Conservation Service. Available online at <https://gdg.sc.egov.usda.gov/>. November 16, 2015 (FY2016 official release).
78. Soil Survey Staff. (1999). Soil Taxonomy A Basis System of Soil Classification for Making and Interpreting Soil Surveys. USDA-NRCS: US Government Printing Office, Washington.
79. Soil Survey Staff. 2014. Keys to Soil Taxonomy, 12th ed. USDA-Natural Resources Conservation Service, Washington, DC.
80. Soil Survey Staff. 2010. Keys to Soil Taxonomy, 11th ed. USDA-Natural Resources Conservation Service, Washington, DC.
81. Soil Survey Staff, 2014. Soil survey laboratory methods manual. Soil Survey Investigations Report, 42. Version 5 NRCS, Washington, DC.

82. Soil Survey Staff and T. Loecke. 2016. Rapid Assessment of Carbon: Methodology, Sampling, and Summary. S. Wills (ed.). US Department of Agriculture, Natural Resources Conservation Service.
83. Strobl, C., Boulesteix, A.L., Zeileis, A. and Hothorn, T., 2007. Bias in random forest variable importance measures: Illustrations, sources and a solution. *BMC bioinformatics*, 8(1), p.25.
84. Stum, A.K., J.L. Boettinger, M.A. White, and Ramsey, R.D. 2010. Random Forests Applied as a Soil Spatial Predictive Model in Arid Utah. p. 179–190. In Boettinger, J.L., Howell, D.W., Moore, A.C., Hartemink, A.E., Kienast-Brown, S. (eds.), *Digital Soil Mapping: Bridging Research, Environmental Application, and Operation*. Springer Netherlands.
85. Szegedy, C., Vanhoucke, V., Ioffe, S., Shlens, J. and Wojna, Z., 2016. Rethinking the inception architecture for computer vision. In *Proceedings of the IEEE Conference on Computer Vision and Pattern Recognition* (pp. 2818-2826).
86. The National Map, 2013. US Department of the Interior, US Geological Survey.
<http://nationalmap.gov/index.html> accessed 06/12/2016.
87. Thompson, J.A., Nauman, T.W., Odgers, N.P., Libohova, Z. and Hempel, J.W., 2012, July. Harmonization of legacy soil maps in North America: status, trends, and implications for digital soil mapping efforts. In *Digital Soil Assessments and Beyond: Proceedings of the Fifth Global Workshop on Digital Soil Mapping* (pp. 97-102).
88. Thompson, J.A., Prescott T., Moore, A.C., Bell, J., Kautz D., Hempel, J., Waltman, S.W. and Perry C.H, 2010. Regional approach to soil property mapping using legacy data and spatial disaggregation techniques. In 19th World Congress of Soil Science, Soil Solutions for a Changing World, Brisbane, Australia.
89. US Census Bureau, Cartographic Boundary Shapefiles - Counties.
https://www.census.gov/geo/maps-data/data/cbf/cbf_counties.html accessed 08/12/2015.

90. Vaysse, K. and Lagacherie, P., 2015. Evaluating digital soil mapping approaches for mapping GlobalSoilMap soil properties from legacy data in Languedoc-Roussillon (France). *Geoderma Regional*, 4, pp.20-30.
91. Walker, P.H., Hall, G.F. and Protz, R., 1968. Relation between landform parameters and soil properties. *Soil Science Society of America Journal*, 32(1), pp.101-104.
92. Waltman, S. W., P. Schoeneberger, D. A. Wysocki, J. A. Thompson, and D. G. Shulze. Soil Landscapes of the United States (SOLUS) – Mapping Soil Parent Material Terms for Educators. Abstract 156-2 SSSA Division: Soil Education and Outreach Poster 1141. ASA, CSSA, SSSA International Annual Meeting, November 2-5, 2014, Long Beach, CA.
93. Warmerdam, F. (2008). The geospatial data abstraction library. In *Open source approaches in spatial data handling* (pp. 87-104). Springer Berlin Heidelberg.
94. Wielemaker, W.G., de Bruin, S., Epema, G.F., Veldkamp, A., 2001. Significance and application of the multi-hierarchical landsystem in soil mapping. *Catena* 43 (1), 15–34.
95. West L., Wills S., Loecke T. Rapid assessment of US soil carbon (RaCA) for climate change and conservation planning. USDA-NRCS, June 2016.
96. Wills, S., Seybold, C., Chiaretti, J., Sequeira, C. and West, L., 2013. Quantifying tacit knowledge about soil organic carbon stocks using soil taxa and official soil series descriptions. *Soil Science Society of America Journal*, 77(5), pp.1711-1723.
97. Wilson, J.P. and Gallant, J.C., 2000. *Terrain analysis: principles and applications*.
98. Wright, M.N., Ziegler, A. 2016. ranger: A Fast Implementation of Random Forests for High Dimensional Data in C++ and R. *Journal of Statistical Software*, p. 18.
99. Wilson, A.M., Jetz, W., 2016. Remotely Sensed High-Resolution Global Cloud Dynamics for Predicting Ecosystem and Biodiversity Distributions. *PLoS Biol* 14(3): e1002415. doi:10.1371/journal. Pbio.1002415

100. Wood, S. N. 2011. Fast stable restricted maximum likelihood and marginal likelihood estimation of semiparametric generalized linear models. *Journal of the Royal Statistical Society: Series B (Statistical Methodology)* 73:3-36.
101. Yokoyama, R., Shirasawa, M. and Pike, R.J., 2002. Visualizing topography by openness: a new application of image processing to digital elevation models. *Photogrammetric engineering and remote sensing*, 68(3), pp.257-266.
102. Zhang, G.L., Liu, F., Song, X.D. and Zhao, Y.G., 2016. Digital Soil Mapping Across Paradigms, Scales, and Boundaries: A Review. In *Digital Soil Mapping Across Paradigms, Scales and Boundaries* (pp. 3-10). Springer Singapore.
103. Zhang, S., Huang, Y., Shen, C., Ye, H. and Du, Y., 2012. Spatial prediction of soil organic matter using terrain indices and categorical variables as auxiliary information. *Geoderma*, 171, pp.35-43.

Table 1. Number of great group observations, great group classes, and observation density in each independent dataset.

| Area Location | Number of Observations | Number of Classes | Observation Density (per km ²) |
|----------------------------|------------------------|-------------------|--|
| Eastern Iowa | 69 | 4 | 2.531 |
| Maine | 183 | 12 | 0.001 |
| Northcentral WY | 51 | 5 | 0.021 |
| Northern MN | 97 | 13 | 0.002 |
| South-central NM | 103 | 5 | 0.026 |
| Southeastern UT | 361 | 9 | 0.006 |
| Western UT (Beaver County) | 326 | 11 | 0.034 |
| Western UT (Juab County) | 204 | 8 | 0.010 |

| | | | |
|-----------------------------|------|----|-------|
| Western UT (Millard County) | 605 | 12 | 0.024 |
| Total | 1999 | | |

Table 2. Number of modified particle size class observations, great group classes, and observation density in each independent dataset.

| Area Location | Number of Observations | Number of Classes | Observation Density (per km ²) |
|-----------------------------|------------------------|-------------------|--|
| Iowa | 69 | 3 | 1.898 |
| Maine | 183 | 14 | 0.001 |
| North-central WY | 51 | 7 | 0.029 |
| Northern MN | 108 | 12 | 0.002 |
| South-central NM | 103 | 8 | 0.042 |
| Southeastern UT | 356 | 7 | 0.005 |
| Western UT (Beaver County) | 329 | 13 | 0.040 |
| Western UT (Juab County) | 208 | 16 | 0.020 |
| Western UT (Millard County) | 605 | 10 | 0.020 |
| Total | 2012 | | |

Table 3 of average prediction error for soil properties based on 10-fold cross-validation. N = “Number of samples used for training”, ME = “Mean Error”, MAE = “Mean Absolute Error”, RMSE = “Root Mean Square Error” and R-square = “Coefficient of determination”.

| <i>Variable Name</i> | <i>N</i> | <i>Mean</i> | <i>Min</i> | <i>Max</i> | <i>ME</i> | <i>MAE</i> | <i>RMSE</i> | <i>R-square</i> |
|----------------------|----------|-------------|------------|------------|-----------|------------|-------------|-----------------|
| Soil organic C | 232,626 | 1.62 | 0.00 | 70.4 | -0.028 | 0.78 | 2.90 | 0.63 |
| % Sand | 189,189 | 34.45 | 0.00 | 99.62 | -0.088 | 7.52 | 11.3 | 0.82 |
| % Clay | 189,189 | 24.12 | 0.02 | 96.5 | -0.131 | 5.88 | 8.70 | 0.72 |
| Bulk Density | 62,764 | 1.38 | 0.06 | 2.6 | -0.002 | 0.11 | 0.16 | 0.66 |
| pH | 194,176 | 6.22 | 2.00 | 10.90 | -0.001 | 0.33 | 0.47 | 0.87 |
| N_total | 74,054 | 0.22 | 0.10 | 5.5 | -0.005 | 0.09 | 0.22 | 0.62 |